The timing of sleep spindles is modulated by the respiratory cycle in humans

Valentin Ghibaudo, Maxime Juventin, N. Buonviso, Laure Peter-Derex

Clinical Neurophysiology xxx (xxxx) xxx

Contents lists available at ScienceDirect

Clinical Neurophysiology

journal homepage: www.elsevier.com/locate/clinph

The timing of sleep spindles is modulated by the respiratory cycle in humans

Valentin Ghibaudo [a], Maxime Juventin [a], Nathalie Buonviso [a,1], Laure Peter-Derex [a,b,1,*]

[a] Lyon Neuroscience Research Centre, INSERM U 1028/CNRS UMR5292, Bron, France
[b] Centre for Sleep Medicine and Respiratory Diseases, Hospices Civils de Lyon, Lyon 1 University, Lyon, France

HIGHLIGHTS

- Sigma activity is enhanced during the expiratory phase of respiration in non-rapid-eye-movement sleep.
- Both slow and fast spindle events occurrence significantly increases during the middle part of the expiration phase.
- Breathing exerts a lower biphasic effect on slow waves occurrence, which increases during respiration phase transitions.

ARTICLE INFO

Article history:
Accepted 28 June 2024
Available online

Keywords:
Sigma
Spindles
Slow waves
Breathing
Coupling
Non-rapid-eye-movement sleep

ABSTRACT

Objective: Coupling of sleep spindles with cortical slow waves and hippocampus sharp-waves ripples is crucial for sleep-related memory consolidation. Recent literature evidenced that nasal respiration modulates neural activity in large-scale brain networks. In rodents, this respiratory drive strongly varies according to vigilance states. Whether sleep oscillations are also respiration-modulated in humans remains open. In this work, we investigated the influence of breathing on sleep spindles during non-rapid-eye-movement sleep in humans.
Methods: Full night polysomnography of twenty healthy participants were analysed. Spindles and slow waves were automatically detected during N2 and N3 stages. Spindle-related sigma power as well as spindle and slow wave events were analysed according to the respiratory phase.
Results: We found a significant coupling between both slow and fast spindles and the respiration cycle, with enhanced sigma activity and occurrence probability of spindles during the middle part of the expiration phase. A different coupling was observed for slow waves negative peaks which were rather distributed around the two respiration phase transitions.
Conclusion: Our findings suggest that breathing cycle influences the dynamics of brain activity during non-rapid-eye-movement sleep.
Significance: This coupling may enable sleep spindles to synchronize with other sleep oscillations and facilitate information transfer between distributed brain networks.

1. Introduction

Sleep spindles are brief (typically 0.5–2 s) bursts of sigma (10–16 Hz) oscillations recorded in the electroencephalogram (EEG) during non-rapid-eye-movement (NREM) sleep. They involve oscillations within reticulo-thalamo-cortical loops and have been associated with cognitive functions including learning and memory (Fernandez and Luthi, 2020). Spindles are synchronized with other NREM sleep oscillations. Indeed, changes in cortical excitability and neuronal firing associated with the phases of NREM slow waves result in an increased probability of spindle during the depolarizing UP-state, and spindles, in turn, cluster hippocampal ripples in their troughs (Contreras and Steriade, 1995, Staresina et al., 2015). The coupling of spindles with cortical slow waves and hippocampus sharp-waves ripples is crucial for triggering reactivation of learning material and promoting hippocampo-neocortical transfer of information in the context of sleep-related

Abbreviations: EEG, Electroencephalogram; E, Expiration; I, Inspiration; Min, minute; N2, Non-rapid-eye-movement sleep stage 2; N3, Non-rapid-eye-movement sleep stage 3; NREM sleep, Non-rapid-eye-movement sleep; RMBOs, Respiration-modulated Brain Oscillations; TF, Time-frequency.

* Corresponding author at: Centre for Sleep Medicine and Respiratory Diseases, Croix-Rousse Hospital, Hospices Civils de Lyon, 103 Grande Rue de la Croix-Rousse, 69004 Lyon, France.
E-mail address: Laure.peter-derex@chu-lyon.fr (L. Peter-Derex).
[1] These authors contributed equally.

https://doi.org/10.1016/j.clinph.2024.06.014
1388-2457/

memory consolidation (Klinzing et al., 2019). Importantly, the precision of slow wave-spindle coupling predicts the learning material reactivation strength, which in turn is predictive of memory consolidation (Schreiner et al., 2021). To note, spindles out of the slow wave UP-state phase are ineffective in improving hippocampus-dependent memory consolidation (Latchoumane et al., 2017). However, not all slow waves are associated with spindles, and some spindles occur outside of slow waves. In addition, other slow and infra-slow rhythms of spindle occurrence have been described (Antony et al., 2018, Lázár et al., 2019, Lecci et al., 2017). It is increasingly likely that such slow rhythms may be linked to the autonomic nervous system activity and bodily rhythms (Azzalini et al., 2019). Thus, a 0.02 Hz oscillation in sigma power has been evidenced, both in mice and humans, resulting from a periodic recurrence of sleep spindles and correlated with cardiovascular activity (Lecci et al., 2017). Similarly, a spindle clustering over periods of 50 sec (0.02 Hz) has been described, during which the frequency of spindle recurrence is around 0.3 Hz, a frequency close to the respiratory frequency (Antony and Paller, 2017).

In such a theoretical framework, it is tempting to posit the respiratory rhythm as one possible candidate to ensure a fine temporal alignment between the different brain activities (cortical slow waves and hippocampus sharp-waves ripples) during sleep (Allen et al., 2023, Brændholt et al., 2023, Folschweiller and Sauer, 2022, 2023, Heck et al., 2019, Heck et al., 2016). In fact, several studies published in recent years have highlighted that the role of respiration goes beyond homeostatic exchange of oxygen and carbon dioxide and that breathing rhythmicity is capable of directly modulating neural oscillations (Heck et al., 2016). Respiration-modulated Brain Oscillations (RMBOs) may result from respiration induced phase-locked changes in neuronal gain and cortical excitability, and involve cross-frequency phase-amplitude coupling phenomena (Brændholt et al., 2023). Thus, respiration was shown to modulate neuronal activity in large-scale subcortical and cortical networks, especially during wake (Kluger and Gross, 2021, Tort et al., 2018).

In rodents, several studies have shown that nasal respiration drives neuronal oscillations into the olfactory bulbs, the piriform cortex, and in downstream regions such as the hippocampus and the neocortex (Girin et al., 2021, Tort et al., 2018). Not only slow oscillations in the delta-theta band, but also high frequency rhythms are modulated by the respiration rate and amplitude [for review, see (Juventin et al., 2023)]. This includes hippocampal sharp-wave ripples, whose occurrence probability increases during the early expiration phase (Liu et al., 2017), and coupling between brain oscillations in different frequency bands such as theta and gamma (Hammer et al., 2021). This respiration-locked effect has also been described in rodents during physiological sleep states (Girin et al., 2021, Hammer et al., 2021, Tort et al., 2021) and during anesthesia, with sleep-like induced slow oscillations in the olfactory bulb and cortex correlating with natural breathing (Fontanini et al., 2003). Recently, respiration was shown to promote the coupling between hippocampal sharp-wave ripples and cortical DOWN/UP state transitions, a neuronal process involved in memory consolidation (Karalis and Sirota, 2022). However, recent findings in mice and cats suggest a dampened influence of respiratory signal on cortical activity in REM and NREM sleep (Basha et al., 2023, Jung et al., 2023). These observations may result from state-related changes in respiration pattern as especially deep and slow breathing was shown to favor brain respiratory drive (Girin et al., 2021, Juventin et al., 2023), or may involve sleep dependent modulation of respiratory inputs and cortical excitability (Basha et al., 2023, Jung et al., 2023).

In humans, studies on RMBOs are less numerous and have focused almost exclusively on the waking state. Several works using intracranial EEG, scalp EEG or Magneto-encephalography (MEG) have reported that natural breathing synchronizes brain activity including oscillations in different frequency bands and the aperiodic component of the signal, over widespread cortical and subcortical areas (Herrero et al., 2018, Kluger et al., 2023, Kluger and Gross, 2021, Watanabe et al., 2023, Zelano et al., 2016). Importantly, such coupling translates in the modulation of various cognitive functions. This has been shown for sensory perception (Grund et al., 2022), motor function (Kluger and Gross, 2020, Rassler and Raabe, 2003), as well as emotions processing (Arch and Craske, 2006, Mizuhara and Nittono, 2023) and higher cognitive functions including memory (Arshamian et al., 2018, Johannknecht and Kayser, 2022, Nakamura et al., 2018, Perl et al., 2019, Zelano et al., 2016) although some findings remain conflicting (Mizuhara and Nittono, 2022). However, to date, no study in humans has focused on the possible respiratory modulation of sleep oscillations including spindles, except a recent one exploring this coupling during a nap (Schreiner et al., 2023). Thus, the issue of a possible differential effect of wake/sleep states on the RMBOs remains open. Here, we aimed at examining whether spindles and slow waves recorded from a full night's sleep could be respiration-modulated in humans. Knowing the different functional roles and properties of fast and slow spindles (Fogel and Smith, 2011, Purcell et al., 2017), we also investigated whether such coupling apply to both spindle types and exhibit topographical specificities.

2. Methods

2.1. Participants

Twenty healthy participants (mean ± SD age 31.6 ± 8.3 years; body mass index 22.1 ± 2.8 kg/m^2, 17 females, 3 males) who had participated in another research project focusing on idiopathic hypersomnia, including a full night polysomnography (PSG) were randomly selected for this study. All participants had benefited from an extended clinical evaluation to rule out possible sleep-related condition, including an interview with a sleep physician and standardized questionnaires (Pittsburgh Sleep Quality Index, Epworth Sleepiness Score, Insomnia Severity Index, Hospital Anxiety and Depression scale, Pichot fatigue scale, Horne and Ostberg morningness-eveningness questionnaire). Exclusion criteria were: any sleep disorders; any medical or psychiatric conditions; any medication or drug known to influence sleep; shift work; sleep deprivation (ruled out by a 7-day actigraphy prior to the PSG). All participants granted informed consent. The study was approved by the Hospices Civils de Lyon Ethics Review Board (N° 22_5757, 10/06/2022).

2.2. Sleep recordings

Night sleep recordings were conducted in the Centre for Sleep Medicine and Respiratory Diseases of Lyon University Hospital between 2017 and 2021. The following signals were recorded with the Deltamed/Natus® acquisition system (sample rate: 256 Hz): EEG (Fp1, Fp2, Fz, C3, C4, Cz, T3, T4, Pz, O1, O2, A1, A2), electro-oculogram, chin and tibialis electromyogram, EKG, nasal airflow (nasal pressure and oronasal thermistor), pulse oximetry, microphone, and respiratory efforts (thoracic and abdominal belts).

2.3. Respiratory recording and processing

Respiratory cycle detection was performed using an algorithm previously described applied on nasal pressure signal (Roux et al., 2006). Briefly, the segmentation of respiratory signal into individual cycles included the following steps. Respiratory signal was first filtered (4th order low-pass, Bessel, 1.5 Hz) for noise

reduction and centered (using median subtraction and division by standard-deviation). The respiration trace thus cleaned was an around-zero oscillatory signal, with positive (inspiration) and negative (expiration) deflections. A critical point of signal analysis was the segmentation of the respiratory signal into individual cycles that was achieved as follows. The zero crossing points of the falling phase of the signal determined the inspiration to expiration transition (I/E points) while the zero crossing points of the rising phase determined the expiration to inspiration transition (E/I points). We therefore obtained a series of individual cycles with inspiratory phases defined by E/I to I/E epochs, and expiratory phases defined by the I/E to E/I ones. On such individual cycles, artifacts were eliminated by rejecting cycle duration values below and above 1 and 15 s, respectively.

2.4. EEG data analysis

2.4.1. Sleep staging

Sleep staging was performed in 30 s epochs using YASA toolbox (Vallat and Walker, 2021), an automated sleep scoring algorithm based on the American Academy of Sleep Medicine recommendations, followed by a visual checking. EEG recordings were re-referenced to the mean of both mastoid signals and analyses were performed on artefact-free signals. N2 and N3 stage epochs were retained for analyses.

2.4.2. Spindle and slow-wave detection

The same toolbox was used for the detection of spindles (12–15 Hz; 0.5–2 s; threshold > 1.5 SD of the root mean square of the sigma-filtered signal; > 0.65 of a moving correlation between original signal and sigma-filtered signal; > 0.2 of relative power defined as sigma power divided by broadband power). Fast and slow spindles were separated through a frequency threshold manually set for each participant according to the bimodal distribution of their frequencies. These thresholds ranged from 12.3 to 13.7 Hz (mean ± SD: 13.15 ± 0.31 Hz, see Fig. 1). Knowing the strong coupling between spindles and sleep slow-waves (Clemens et al., 2007), we also investigated whether the latter were coupled to respiration. Hence, we also used YASA toolbox to detect slow waves based on the following criteria: a negative deflection of the EEG signal preceding a positive deflection, providing an oscillation of 0.2 to 1.5 Hz, 0.3 to 1.5 s duration for negative deflection and 0.1–1 s duration for positive deflection, peak-to-peak amplitude 75–350 μV.

2.4.3. From timestamps of spindle/slow-wave to corresponding respiratory phase angles

The previously described detection criteria allow YASA algorithm to provide spindles and slow-waves features (timestamps, amplitudes). Timestamps corresponding to spindle onsets and slow wave negative peak times were retained for subsequent analysis. Spindle onsets correspond to the timing when the root mean square of the sigma-filtered signal, the moving correlation sigma filtered to original signal and the relative sigma power all cross their set threshold. These timestamps were converted into phase angles according to the relative time of occurrence during their corresponding breathing cycle, following this equation: ((Spindle onset time − Respiratory cycle starting time) / Respiratory cycle duration) * 360. This method is an equivalent of a linear interpolation.

2.4.4. Sigma power extraction

Time-frequency (TF) maps of the NREM sleep signal were obtained using Complex Morlet Wavelet convolutions. Morlet wavelet settings were optimized to capture spindle-related sigma power of the signal as a function of time (frequencies linearly increasing from 10 to 16 Hz in 60 steps, 20 oscillations, tapering to zero, 4 s duration).

2.4.5. From sigma time–frequency maps to sigma respiratory phase-frequency maps

TF maps were then sliced into epochs according to onset and offset of each respiratory cycle. TF maps corresponding to each of these epochs were then "stretched" as explained in Roux et al. (2006), before making a time-to-phase conversion of the matrices. Briefly, the time component of these epochs, which can differ from trial to trial, was converted into a phase component defined as [0,144°] and [144°, 360°] for inspiration and expiration, respectively, setting a respiratory transition at 40% of the phase vector (144° = 0.4 * 360°). We chose this ratio inspiration / expiration based on the respiratory data: the average proportion of inspiration duration against total cycle duration from the 20 participants was equal to 0.42, meaning 42% of inspiration and 58% of expiration (see Table S1 of supplementary material), which is consistent with physiological data in humans (West and Luks, 2020). As opposed to time representation, the phase representation is common to all epochs regarding the phase axis. Thus, this phase representation of the respiratory cycle is used as a normalized time basis allowing to collect results in a standardized data format across different participants and providing a way to average oscillatory components of the activity (See **Fig. S1** of supplementary material for a graphical explanation of the phase-frequency pipeline). Each phase-frequency map corresponds to one respiratory cycle. This allowed us to select phase-frequency maps according to the presence or not of spindles detected by the YASA toolbox (see Section 2.4.2 and 2.4.3) during the correspond respiratory epoch (see Section 2.3). Thus, phase-frequency maps containing at least one detected spindle were averaged, allowing spindle related sigma power representation.

2.5. . Statistical analysis

Angular values of each population of events (spindles or slow-waves) were pooled from the 20 participants. Circular statistics were computed on each population of angles (spindles onsets or slow-wave negative peaks) providing three types of information. First, angular values (or direction) in the complex domain were extracted and the angle of the mean vector was calculated. Mean angle ranged from 0 to 360°: 0° being the start of a respiratory cycle (meaning the start of an inspiration) and 360° being the end of the respiratory cycle (meaning the end of expiration). Second, the mean vector length was computed taking absolute value of the mean vector, providing an effect size of the non-uniform distribution of the angles toward a preferred direction. Lastly, significance of the non-uniformity of the distribution of angles along respiration phase was assessed by using Hermans-Rasson test. Hermans-Rasson test is an equivalent alternative to the commonly used Rayleigh test to assess non-uniformity of a unimodal angular distribution but outperforms this latter in case of multimodal situation (Landler et al., 2019). The following process was used to obtain a p-value. First, the value of the Hermans-Rasson test was calculated for an original sample of angles. We then drew a number m (1000) of pseudo-samples, each of size n (the size of the original sample) from a uniform distribution on [0,360°]. We then calculated the value of the statistic test for each of these pseudo-samples. We next calculated the number of pseudo-samples that gave a test statistic value of equal or greater magnitude than that of the original sample, called number Q. The p-value of the test was given by (Q + 1)/(m + 1), which leads to a p-value of 0.00099 when all the test values from the pseudo-samples are lower than those of the original sample. We chose to randomly down-sample the initial angle dataset to N = 10000 samples in cases where the original sample size exceeded

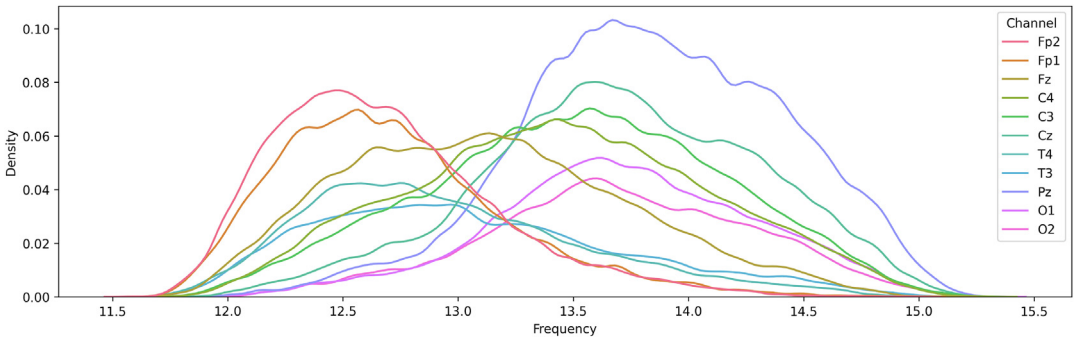

Fig. 1. Spindle frequency distribution according to channel localization (N = 101857 pooled from 20 participants, in N2 + N3 sleep stages). The bimodal distribution distinguishes between anterior slow spindles (12–13 Hz: Fp1, Fp2, T3, T4) and posterior fast spindles (13–15 Hz: Pz, C3, C4, O1, O2). Fz records both slow and fast spindles (green khaki). (For interpretation of the references to colour in this figure legend, the reader is referred to the web version of this article.)

10000 to reduce computation time while allowing sufficient statistical power to reject the null hypotheses (uniformity of distribution) when less that 50 over 1000 of the pseudo-samples have a higher p-value that the original sample.

3. Results

3.1. Sleep features

On average, 231 ± 31 min of N2 epochs and 80 +/- 23 min of N3 epochs per participant were used for analyses. Sleep parameters are presented in Table 1. Considering all channels (n = 11 per participant) in NREM (N2 + N3 combined), 5772 ± 2899 spindles were detected per participant (density = 1.2 ± 1.5 spindles per minute per channel per participant) with a 0.88 ± 0.30 s mean duration and a 13.37 ± 0.71 Hz mean frequency. A total of 11637 ± 6126 slow waves were detected per participant, with a 1.20 ± 0.30 s mean duration, a 0.88 ± 0.21 Hz mean frequency, and a negative-to-positive peak mean amplitude of 130 ± 47 μV. Spindle frequency distribution according to channel localization showed a bimodal distribution with slow spindles (12–13 Hz) predominant in fronto-temporal channels and fast spindles (13–15 Hz) predominant in centro-parieto-occipital channels, whereas Fz recorded both fast and slow spindles (Fig. 1).

3.2. Respiration features

Considering N2 + N3 sleep stages, participants respiration cycles lasted on average 3.73 ± 0.44 s corresponding to 1.56 ± 0.1 9 s of inspiration and 2.17 ± 0.29 s of expiration (in N2: 3.77 ± 0. 45 s corresponding to 1,57 ± 0.18 s of inspiration and 2.19 ± 0.30 s of expiration.; in N3: 3.63 ± 0.41 s corresponding to 1.54 ± 0.21 s of inspiration and 2.09 ± 0.28 s of expiration). Detailed respiration features computed during NREM sleep for each participant are presented in **Table S1** of supplementary material.

3.3. Spindle-related sigma power coupling with respiration

Spindle related sigma power was extracted using Morlet Wavelet convolutions and computed along the respiration cycle phase. As evidenced by the mean respiratory phase-frequency map of sigma band power in NREM sleep (Fig. 2**A**), the power was not evenly distributed over the respiratory cycle but was higher during the expiratory phase for all the channels. This was observed both in N2 and N3 sleep stages (Fig. 2**B and 2C**). Individual maps performed in each channel revealed that it was true for most of the 20 participants (See Fig. 2**D** for Fz and **Fig. S2** of supplementary material for all other channels). Nevertheless, some inter-individual variability appeared in the phase, frequency and/or duration of the sigma peaks. In some participants and channels, a double band was observed in the sigma power, indicating non-overlapping slow and fast spindle-related sigma frequencies.

3.4. Spindles and slow waves events coupling with respiration

Given the results obtained from the time–frequency maps, and in order to increase the number of events and perform sub-group analyses, N2 and N3 stages were pooled for the following analyses. When considering the probability of occurrence of spindle events detected on the different channels as a function of the respiratory cycle, Hermans-Rasson test underlined a non-uniform distribution for spindles onsets (p-value < 0,001; N = 20 participants). The mean direction indicated a significantly increased probability during the expiration phase with a mean vector length of 0.086 and an angle of 266° of respiration phase (Fig. 3**A**, grey polar distribution). Since NREM spindles have been described as phase-locked to sleep slow waves, we explored if slow waves were also respiration-phased. Polar plots of slow waves negative peaks revealed that they were not as non-uniformly distributed as spindles but a significant increase of probability of occurrence was still observed around both respiration transition phases (inspiration to expiration and expiration to inspiration, $p < 0.05$) (Fig. 3**A**, green polar distribution). Given the different functional role of slow compared to fast spindles, we analysed separately these two spindle populations. The significant increase of spindles during expiration phase was confirmed for both slow and fast spindles ($p < 0.001$ for both types) (Fig. 3**B**): the mean vector lengths were 0.081 and 0.092 with a mean angle of 276° and 255° for the slow and fast spindles respectively. Results obtained in other channels are presented in Fig. 3**C** and the corresponding circular statistics are provided in Table S2 of supplementary material, showing that fast spindles slightly precede slow spindles along the respiratory cycle in all investigated regions except in the occipital areas, where very few slow spindles are detected. Finally, we investigated whether this coupling was modulated by homeostasis, as sleep spindles density were described to fluctuate across the night with a differential effect for slow and fast spindles according to the age (Purcell et al., 2017). To explore this question, we separately analysed recordings from the four successive quartiles of the night (Fig. 4). We found no significant differences between the four quartiles for the strength and direction of coupling between spindles (slow or fast) or slow-waves with respiration phase (see Table S3 of supplementary material for circular statistics), all being non-uniformly distributed ($p < 0.05$).

4. Discussion

We found a significant coupling between sleep spindles and the respiration cycle, with enhanced sigma activity as well as slow and

Table 1
Sleep parameters during the recorded night- Sleep parameters have been computed for each participant (S1 to S20). Mean and standard deviations (SD) are presented in the last two rows. All units are minutes or percentages (% in columns labels). Abbreviations: Time in Bed (TIB): total duration of the file; Total Sleep Period (TSP): duration from first to last epoch of sleep.; Wake After Sleep Onset (WASO): duration of wake periods within TSP; Total Sleep Time (TST): total duration of N1 + N2 + N3 + R sleep in TSP; Sleep Efficiency (SE): TST / TIB * 100 (%); Sleep Maintenance Efficiency (SME): TST / TSP * 100 (%); W, N1, N2, N3 and R: sleep stages duration. NR = N1 + N2 + N3; % (W, . . . R): sleep stages duration expressed in percentages of TST; Sleep Onset Latency (SOL): Latency to first epoch of any sleep stage.

Participant	TIB	TSP	WASO	TST	N1	N2	N3	R	NR	SOL	%N1	%N2	%N3	%R	%NR	%SE	%SME
P1	527.5	440	32.5	407.5	30	190.5	64.5	122.5	285	51.5	7.36	46.75	15.83	30.06	69.94	77.25	92.61
P2	560.5	520	45	475	29.5	242.5	83	120	355	40.5	6.21	51.05	17.47	25.26	74.74	84.75	91.35
P3	598.5	580.5	43.5	537	36	290.5	73.5	137	400	18	6.7	54.1	13.69	25.51	74.49	89.72	92.51
P4	524.5	503.5	51.5	452	61	241	50	100	352	14.5	13.5	53.32	11.06	22.12	77.88	86.18	89.77
P5	498.5	488	50	438	53.5	216	63.5	105	333	10.5	12.21	49.32	14.5	23.97	76.03	87.86	89.75
P6	509	474	44	430	45.5	201	109.5	74	356	35	10.58	46.74	25.47	17.21	82.79	84.48	90.72
P7	523	469.5	53	416.5	29.5	219.5	84	83.5	333	53.5	7.08	52.7	20.17	20.05	79.95	79.64	88.71
P8	430	421.5	73.5	348	40.5	177.5	45	85	263	8.5	11.64	51.01	12.93	24.43	75.57	80.93	82.56
P9	542	537.5	40	497.5	14.5	289	72	122	375.5	4.5	2.91	58.09	14.47	24.52	75.48	91.79	92.56
P10	535	483	83	400	31.5	220	68.5	80	320	32.5	7.88	55	17.12	20	80	74.77	82.82
P11	430.5	417	42	375	13.5	185	68.5	108	267	13.5	3.6	49.33	18.27	28.8	71.2	87.11	89.93
P12	539	501.5	89.5	412	52	214	36	110	302	15	12.62	51.94	8.74	26.7	73.3	76.44	82.15
P13	468.5	448.5	17.5	431	23.5	220	98	89.5	341.5	20	5.45	51.04	22.74	20.77	79.23	92	96.1
P14	578	535	29	506	39.5	253.5	82	131	375	43	7.81	50.1	16.21	25.89	74.11	87.54	94.58
P15	528.5	517.5	32	485.5	26.5	241	107.5	110.5	375	11	5.46	49.64	22.14	22.76	77.24	91.86	93.82
P16	473.5	458.5	8	450.5	11	232.5	95	112	338.5	15	2.44	51.61	21.09	24.86	75.14	95.14	98.26
P17	548	518.5	22	496.5	29.5	256.5	70.5	140	356.5	21	5.94	51.66	14.2	28.2	71.8	90.6	95.76
P18	575.5	566	60.5	505.5	32	254	103.5	116	389.5	9	6.33	50.25	20.47	22.95	77.05	87.84	89.31
P19	574.5	558.5	64.5	494	26	212.5	114	141.5	352.5	16	5.26	43.02	23.08	28.64	71.36	85.99	88.45
P20	533	509.5	16.5	493	29	255	107.5	101.5	391.5	23.5	5.88	51.72	21.81	20.59	79.41	92.5	96.76
Mean	524.8	497.4	44.88	452.5	32.7	230.5	79.8	109.4	343.0	22.8	7.34	50.92	17.57	24.16	75.84	86.22	90.92
SD	46.13	46.44	21.85	50.03	13.14	30.99	22.6	20.05	39.41	14.71	3.2	3.2	4.46	3.41	3.41	5.8	4.58

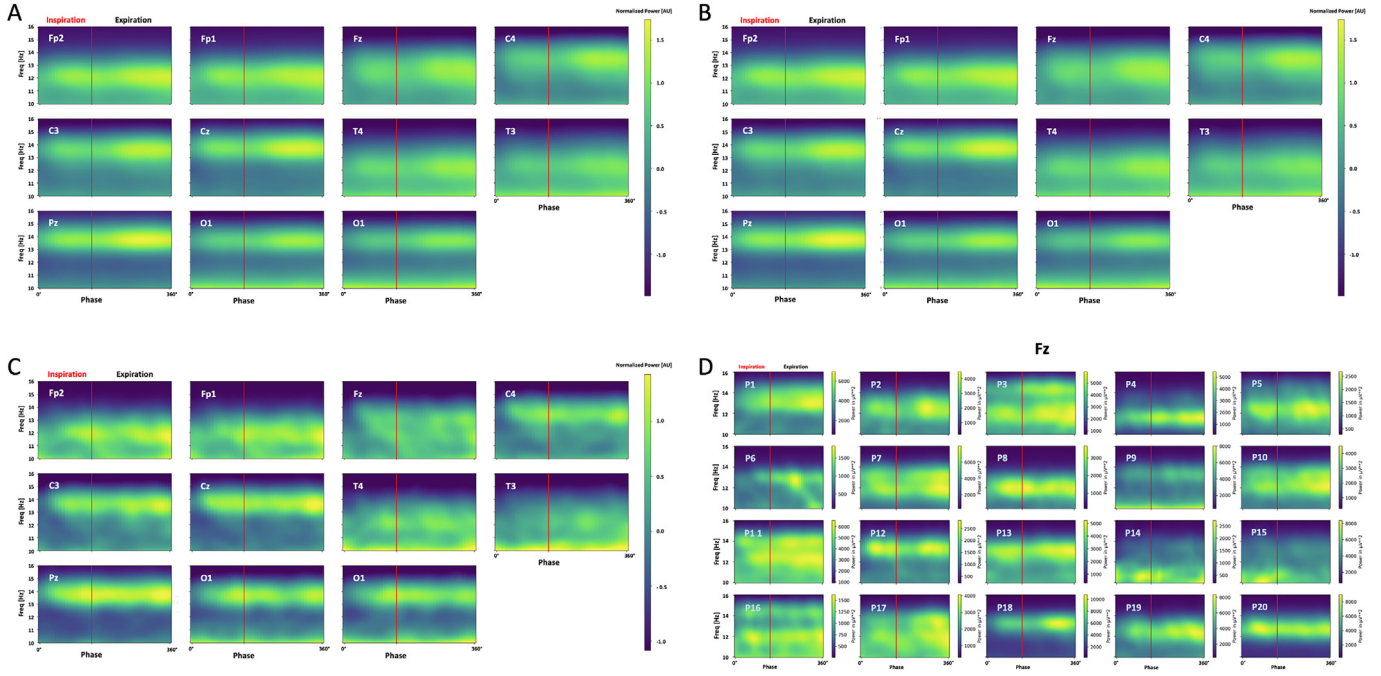

Fig. 2. Spindle related sigma power according to respiration phase Sigma power is higher during the expiratory phase. Respiration phase is expressed in degree from 0° to 360°, beginning from inspiration and ending before the next inspiration. Red vertical line shows the transition point between inspiration and expiration. **A to C.** Mean respiratory phase-frequency map sigma band power (n = 20 participants) in all channels in NREM N2 + N3 stages (**A**), as well as in N2 (**B**) and N3 (**C**) stages separately. Power matrix of each participant and channel has been z-scored before averaging. Note that spindle frequency is lower in anterior (Fp1, Fp2) than in posterior (C3, C4, Cz, Pz) channels. **D.** Individual phase-frequency maps of Fz channel sigma band power. Note the double band representation of the sigma power for some participants (such as P3 and P11), due to the non-overlapping of slow versus fast spindle-related sigma frequencies. Individual maps for all localizations are provided in Fig. S1 of supplementary material. (For interpretation of the references to colour in this figure legend, the reader is referred to the web version of this article.)

fast spindle events during the second part of the expiration phase, while slow waves DOWN states were locked with respiration transition phases (inspiration to expiration and expiration to inspiration). These results show that sleep oscillations are modulated by breathing in humans.

4.1. Respiratory modulation of brain oscillations in humans during wake and sleep

Whereas several works have provided evidence that the nasal respiration drive neuronal oscillations not only in olfactory areas

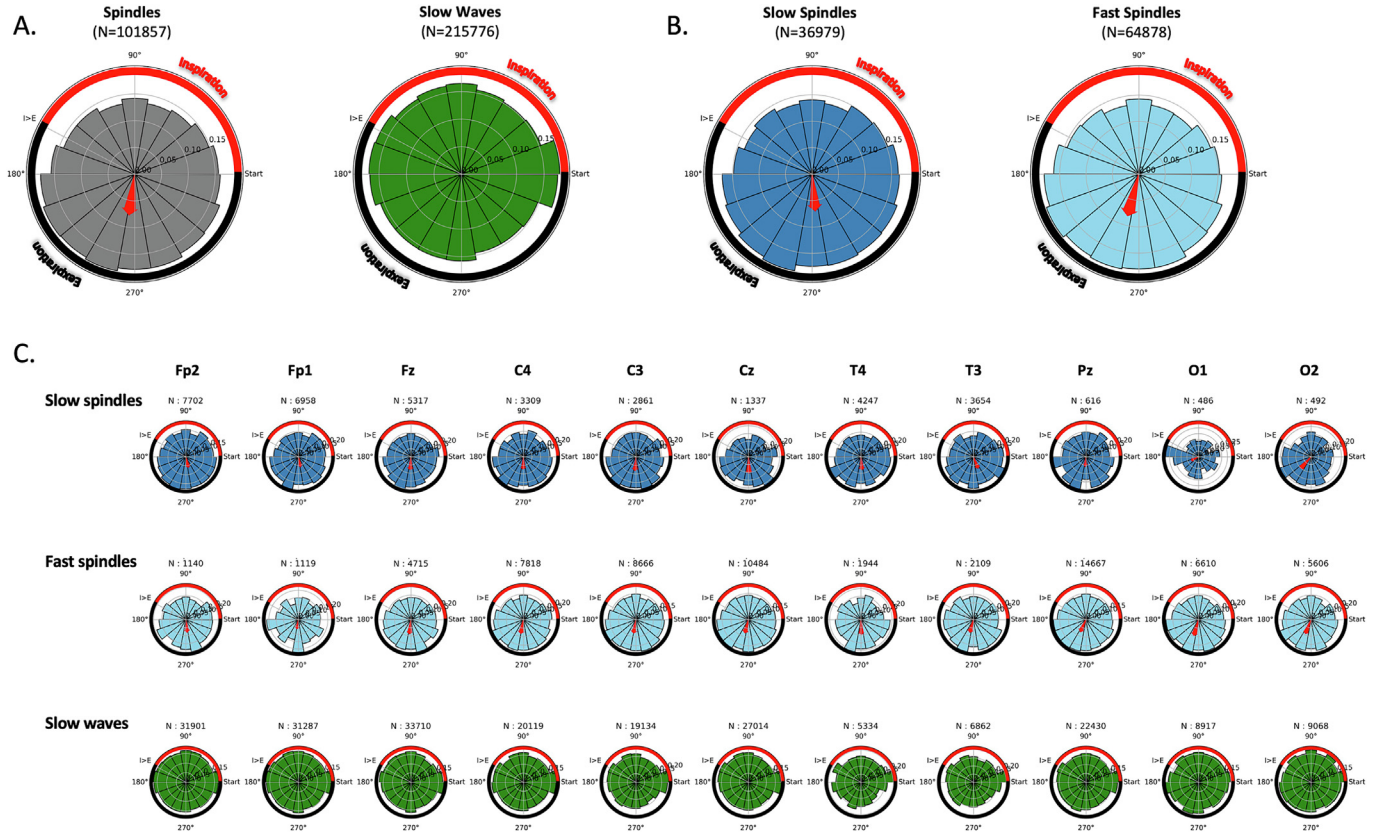

Fig. 3. Spindle and slow waves events occurrence according to respiration phase. Spindle onsets and slow-wave negative peaks were considered as timing events. Timing events from the 20 participants were pooled. These events were labelled with the phase angle of occurrence according to breathing cycle and distributed in 18 equal phase bins of respiration (20° per bin). The count of events distributed is presented in title (N). Inspiration and expiration phases are indicated by the red and black lines respectively. A red arrow indicates the mean angular direction in case of unimodal distribution, and its length depends on the resultant mean vector length that is represented on the circular ticks. **A.** Polar distribution of spindles (grey) and slow wave (green) events according to respiratory cycle. Mean vector lengths is equal to 0.086 and the angle is 266° for spindles, while the distribution of slow waves negative peak is bimodal, pointing toward the respiratory transitions. **B.** Polar distribution of slow spindles (dark blue) and fast spindles (light blue) events according to respiratory cycle. Mean vector lengths are equal to 0.081 and 0.092 for the slow and fast spindles polar distributions, respectively. **C.** Polar distribution of slow spindles (dark blue), fast spindles (light blue) and slow wave (green) for each channel events according to respiratory cycle. Circular statistics for each channel are presented in **Table S2** of supplementary material. All distributions presented in A, B and C are significantly non-uniform as assessed by Hermans-Rasson test (p-value < 0.05). Globally, slow and fast spindles occurrence is higher during the expiration phase while slow waves are more distributed near respiration phase transitions (inspiration to expiration and expiration to inspiration). (For interpretation of the references to colour in this figure legend, the reader is referred to the web version of this article.)

but also in the hippocampus and the neocortex during wake and sleep states in rodents, none of these studies focused on the respiratory modulation of sleep spindles (Girin et al., 2021, Ito et al., 2014, Juventin et al., 2022, Liu et al., 2017, Tort et al., 2018, Tort et al., 2021). In human, most studies on breathing effect on neural rhythms have focused on the wake state. In seven patients with epilepsy explored with intracranial EEG, natural breathing was reported to synchronize electrical activity during the inspiration peak in delta, theta and beta frequency bands in the piriform cortex, amygdala and hippocampus (Zelano et al., 2016). These findings were extended to widespread cortical areas and to gamma oscillations (Herrero et al., 2018). Recently, MEG recordings have allowed to identify respiration-modulated brain oscillations from 2 to 150 Hz within a widespread network of cortical and subcortical brain areas at rest (Kluger and Gross, 2021) and significant coherence between local field potential and respiration signals was found using scalp EEG recordings (Watanabe et al., 2023). However, only one recent work has investigated the influence of respiration cycle on oscillations in the human sleeping brain (Schreiner et al., 2023). The authors analyzed N2 + N3 sleep stages during an afternoon nap in 20 individuals and found enhanced slow wave and spindle frequency power as well as increased slow waves, spindles and coupled slow-wave_spindles events around the inhalation peak. Using combined phase/frequency and event-locked analyses on full night polysomnography, which allowed to base our analyses on a large number of events, we show that sleep spindles are coupled with the expiratory phase of the respiration and that this coupling is consistent across brain regions, spindle type (slow vs fast) and night periods, with a high within and between participants reproducibility. In addition, slow waves DOWN states occurrence was found to increase during transitions between respiration phases (Fig. 5). Our findings thus confirm the influence of breathing on the timing of phasic oscillations in NREM night sleep, although its contribution to sleep-related oscillations synchronization including ripples, and its possible factors of modulation such as circadian regulation and homeostasis including prior wakefulness duration, would need to be further investigated.

4.2. Mechanisms involved in respiration driven modulation of brain oscillations

During wakefulness, local field potential activity in limbic area including the piriform cortex, the amygdala, and the hippocampus, is entrained by nasal breathing, disappearing with oral breathing (Zelano et al., 2016). This suggests that the respiration-locked effect may be driven by the mechano-sensitivity of olfactory sen-

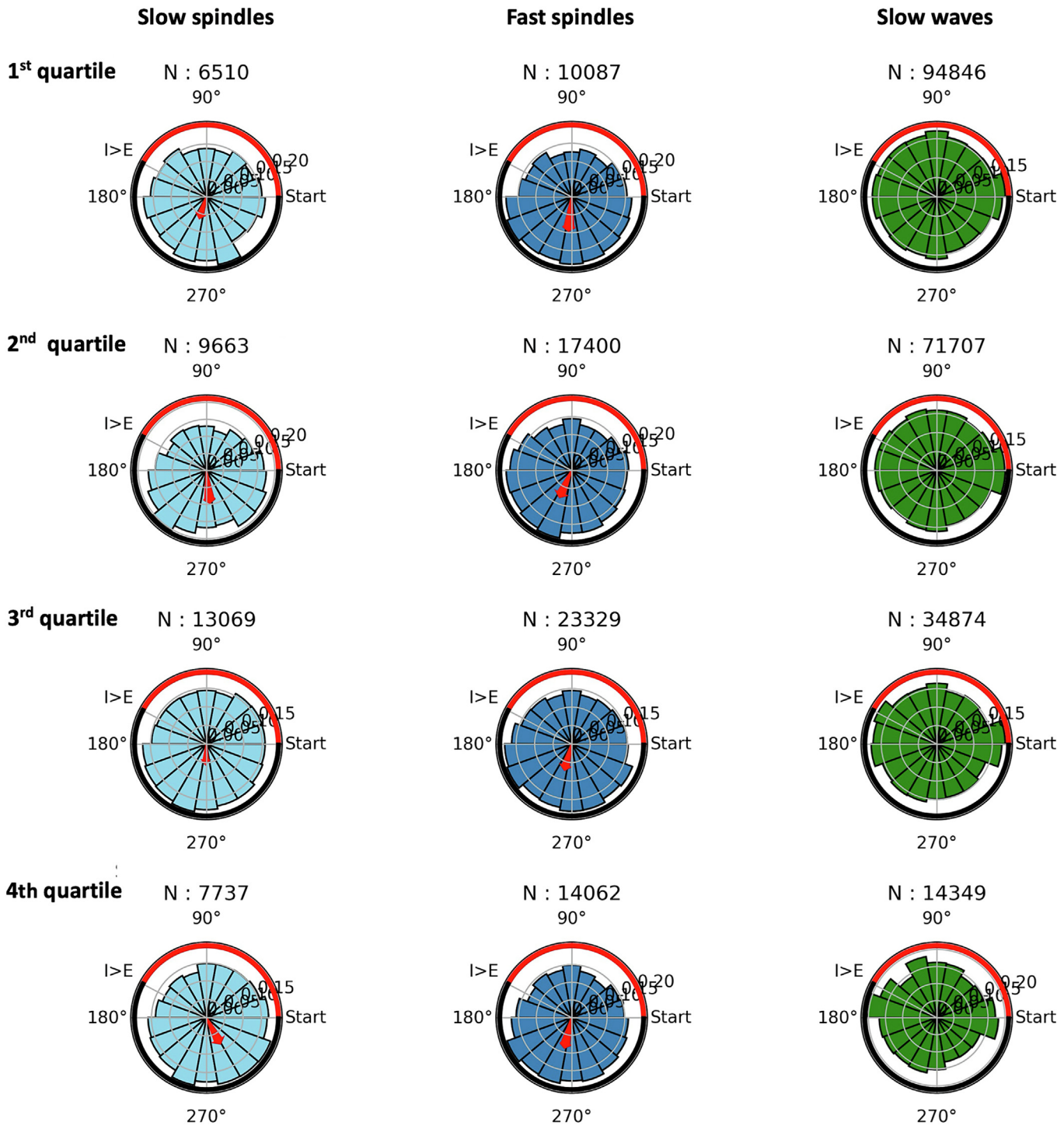

Fig. 4. Spindle and slow waves events occurrence according to respiration phase for the four quartiles (q1 to q4) of the night. Spindle onset (blue) and slow-wave negative peak (green) times from all channels pooled from 20 participants were distributed along the respiration phase. The number of events distributed is presented in title (N). Inspiration and expiration phases are indicated by the red and black lines respectively. A red arrow indicates the mean angular direction, and its length depends on the resultant mean vector length that is represented on the circular ticks. (For interpretation of the references to colour in this figure legend, the reader is referred to the web version of this article.)

sory neurons to air pressure (Grosmaitre et al., 2007), with olfactory bulb responses propagating to other brain area and promoting faster oscillations (Girin et al., 2021, Ito et al., 2014, Juventin et al., 2023, Zelano et al., 2016). During sleep however, a recent study in mice revealed that respiratory modulation of sharp wave ripples occurrence and up/down states is maintained after olfactory deafferentation, suggesting the existence of an ascending respiratory corollary discharge, likely propagating from the brainstem (Karalis and Sirota, 2022). This ascending pathway may involve projections from the pre-Bötzinger complex to brainstem and suprapontine structures (Yang and Feldman, 2018). In particular, projections to the locus coeruleus, whose efferences modulate the excitability of widespread subcortical (including thalamic) and cortical regions, may play a key role in breathing influence

on arousal and information processing during wake and sleep (Beas et al., 2018, Lecci et al., 2017, Yackle et al., 2017). Another mechanism may be the direct transduction of pression fluctuations associated with respiration rhythm to the cortex via mechanosensitive channels present in cortical pyramidal cells (Jung et al., 2022, Nikolaev et al., 2015). These mechanisms, which are not exclusive, might lead to the rhythmic modulation by breathing of local and global gain at the cortical level (Allen et al., 2023). Interestingly, long-range coherence between the medial prefrontal cortex and the nucleus reuniens of the thalamus, phase locked with respiration, was recently reported in cats, although restricted to the wake state; the authors suggested that this rhythm was driven by the entorhinal cortex which receives inputs from the piriform cortex and projects to the nucleus reuniens (Basha et al., 2023), enlightening the role of the olfactory pathway in this influence.

Extensive data have highlighted the persistence of brain responses to various sensory inputs during sleep (Bastuji and García-Larrea, 1999). Lechinger et al reported that heartbeat evoked responses were also modulated by sleep state (Lechinger et al., 2015). Importantly, in addition to eliciting a specific time-locked response, interoceptive signals could have the potential to shape background brain activity. Thus, the authors found a temporal coupling between heartbeats and sleep oscillations (slow waves and spindles) (Lechinger et al., 2015). Our results reveal that breathing is also able to influence brain activity during NREM sleep in thalamo-cortical networks in humans. To note, slow and fast spindles exhibited close strength and phase of respiratory coupling, suggesting a widespread effect of respiration on cortical excitability and neuronal oscillations throughout the brain (Herrero et al., 2018). However, a constant phase advance of fast spindles in relation to slow spindles was observed, which is consistent with the temporal delay (200 msec) previously described between for slow versus fast spindles (Andrillon et al., 2011). We also found a lower biphasic breathing effect on slow waves occurrence, suggesting that the oscillations between cortical UP and DOWN states may also partly depend on respiration phase transitions. The relative contribution of nasal vs ascending respiratory activity should however be further investigated.

4.3. Function and role of brain oscillations shaping by interoceptive signals

The recent concept of "embodied cognition" posits that the body, as an ensemble of fluctuating systems nested at different time scales (heartbeat, respiration, gastric rhythm etc.), modulates brain functioning (Allen et al., 2022, Azzalini et al., 2019, Foglia and Wilson, 2013). This includes notably the influence of interoceptive afferences on motor activity, perception, emotions, and memory (Heck et al., 2022, Varga and Heck, 2017). The functional role of visceral inputs may be related to allostasis, which requires informing the brain of the body states in order to adjust several functions and behaviors to anticipate future needs. Bodily signals might also be involved in the subjective perception of the environment, the sense of body-self, the first-person perspective, and inner mental states (Azzalini et al., 2019). It was also proposed that they might allow adjusting arousal level and information processing across individuals (Parviainen et al., 2022, Sliwa, 2021). Although the influence of heartbeat on brain activity including heartbeat evoked potentials and oscillatory activities has been demonstrated several years ago (Lechinger et al., 2015, Pollatos and Schandry, 2004) evi-

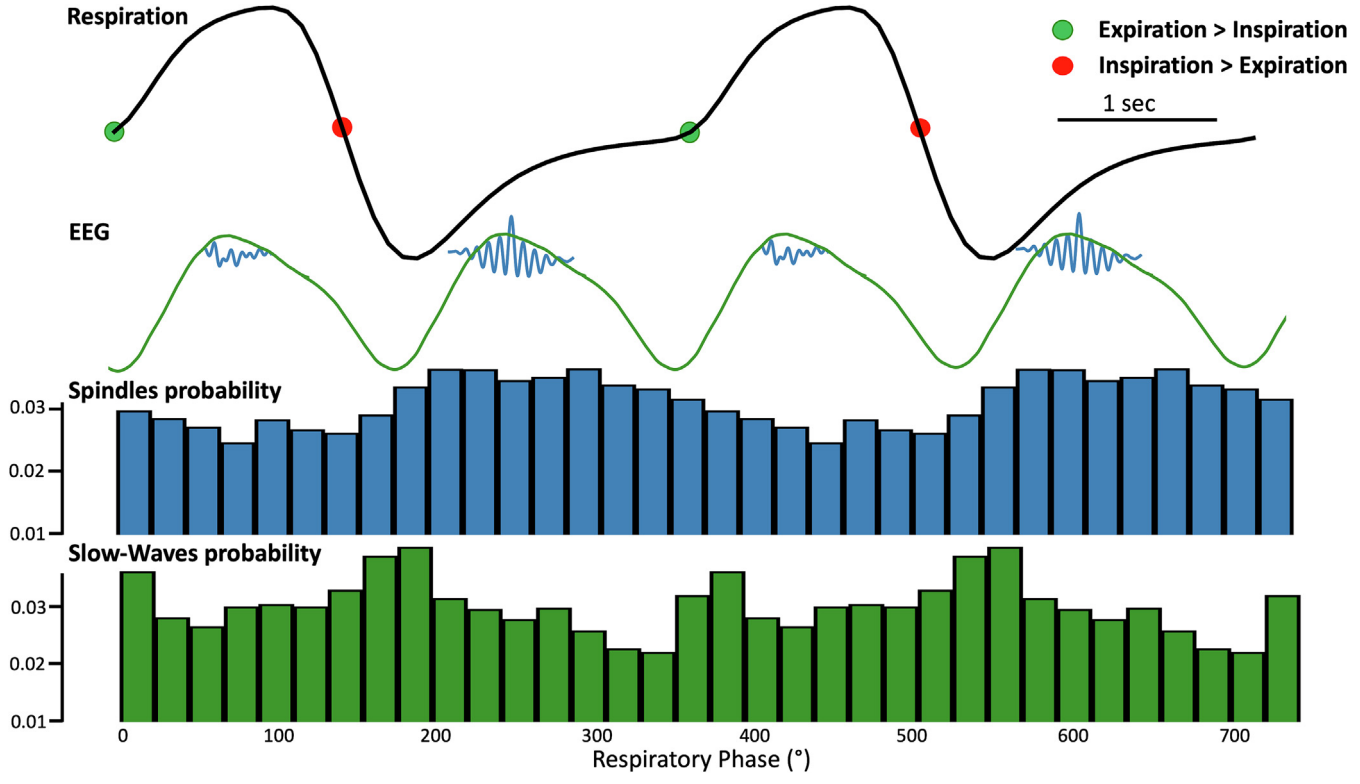

Fig. 5. Representation of the temporal relationship between the respiration cycle, slow waves and spindles. Top traces are representative of a mean typical respiratory signal (black trace) and slow-wave activity (green trace). Typical spindles are represented as blue traces superimposed on the slow-wave trace. Histograms of spindles (blue) and slow-waves (green) probability are based on the distribution of events in Fz (all participants, N2 + N3 sleep stages) (y scale: N of events per bin / total number of events; x scale; phase or the respiratory cycle in °). Negative peaks corresponding to DOWN states of slow waves (green) are phase-locked with respiration transition (expiration to inspiration and inspiration to expiration). However, only UP states occurring during expiration are associated with and increased probability of spindles (blue). (For interpretation of the references to colour in this figure legend, the reader is referred to the web version of this article.)

dence that the breathing cycle may also regulate cortical excitability and coordinate neuronal activity was only provided recently, and almost exclusively during wake state.

We observed that slow and fast sleep spindles were locked to the expiratory phase. This effect, potentially linked to changes in cortico-subcortical excitability along the respiratory cycle, might participate in the post-spindle refractoriness proposed to protect memory reprocessing from interference and optimize oscillatory interactions across regions (Antony et al., 2018). It may also be involved in the clustering of spindles with a 3–6 s period, which has been hypothesized to allow timed reactivation of learning material and favor hippocampo-subcortico-neocortical transfer of information (Boutin and Doyon, 2020, Boutin et al., 2022, Klinzing et al., 2019). The phase amplitude coupling (PAC) is indeed a key mechanism to coordinate neuronal activity over distant areas, promoting local computation, information transfer from large-scale brain networks and synaptic plasticity (Bonnefond et al., 2017, Canolty and Knight, 2010, Fell and Axmacher, 2011). During sleep, respiration may thus increase the precision of slow wave-spindle-ripples coupling, which is crucial for sleep-related memory consolidation (Latchoumane et al., 2017, Schreiner et al., 2021).

4.4. Limitations

We acknowledge several limitations to the study. First, this was an exploratory study on a limited number of participants, with a high proportion of young women (participants were healthy controls selected from a study on idiopathic hypersomnia). This limits the generalisability of our results, which will need to be confirmed in larger cohorts of subjects of various ages with more balanced sex ratio as age-dependant and sex-dependant specificities in spindles have been reported (Purcell et al., 2017). Importantly, we could not control for menstrual cycle phase as this study was retrospective; given the role of estrogen and progesterone levels in sleep spindles and respiration modulation, further studies are needed to specifically investigate this question (Driver et al., 1996, Macnutt et al., 2012). Second, as only one night was recorded in the participants, we cannot rule out a possible first-night effect, although this effect seems less pronounced in younger individuals and does not appear to involve N2 to a significant extent (Ding et al., 2022). Third, we chose to use a narrow frequency band (12–15 Hz ± 1.5 Hz of transition bandwidth) for spindle detection in order to increase the specificity of detections. Visual countercheck of automatic spindle detections in a subset of participants showed a 75% sensitivity and 96% positive predictive value, meaning few false positive but a significant amount of false negative, which may have impeded statistical power, as only automatically detected spindles were kept for the analysis. Last, we conducted a retrospective, non-interventional study with no behavioral/cognitive data; thus, our results do not allow us to demonstrate the causality of the link between breathing and slow wave sleep oscillations, nor to investigate the cognitive role potentially associated with this breathing-brain coupling.

5. Conclusion

Respiration phase influences the dynamics of brain activity during NREM sleep, suggesting a contribution of interoceptive afferences to brain functioning during sleep. We observed that slow waves DOWN states occur predominantly during respiratory transition phases, but that spindles occur mainly during expiratory UP states (Fig. 5). This body-brain coupling may modulate sleep-related cognition, paving the way for neuromodulation approaches targeting respiration. The impact of breathing characteristics on sleep-related cognitive functions, as well as the consequences of sleep-related breathing disorders and mechanical ventilation on this breath-to-brain effect remain to be investigated.

Data and code sharing statement

The data that support the findings of this study are available from the corresponding author upon reasonable request. The python codes used for the current study are available here: https://github.com/ValentinGhibaudo/Sleep_EEG_Respi.

Funding

This research did not receive any specific grant from funding agencies in the public, commercial, or not-for-profit sectors.

Author contribution

Design of the study: VG, LPD and NB; Data collection: LPD; Data analysis: VG, MJ; Results interpretation: VG, LPD and NB; Manuscript drafting and reviewing: VG, LPD, MJ and NB.

Conflict of interest

None.

Appendix A. Supplementary material

Supplementary material to this article can be found online at https://doi.org/10.1016/j.clinph.2024.06.014.

References

Allen M, Levy A, Parr T, Friston KJ. In the body's eye: the computational anatomy of interoceptive inference. PLoS Comput Biol 2022;18(9):e1010490.
Allen M, Varga S, Heck DH. Respiratory rhythms of the predictive mind. Psychol Rev 2023;130(4):1066–80.
Andrillon T, Nir Y, Staba RJ, Ferrarelli F, Cirelli C, Tononi G, et al. Sleep spindles in humans: insights from intracranial EEG and unit recordings. J Neurosci 2011;31(49):17821–34.
Antony JW, Paller KA. Using oscillating sounds to manipulate sleep spindles. Sleep 2017;40(3).
Antony JW, Piloto L, Wang M, Pacheco P, Norman KA, Paller KA. Sleep spindle refractoriness segregates periods of memory reactivation. Curr Biol 2018;28(11):1736–1743.e4.
Arch JJ, Craske MG. Mechanisms of mindfulness: emotion regulation following a focused breathing induction. Behav Res Ther 2006;44(12):1849–58.
Arshamian A, Iravani B, Majid A, Lundstrom JN. Respiration modulates olfactory memory consolidation in humans. J Neurosci 2018;38(48):10286–94.
Azzalini D, Rebollo I, Tallon-Baudry C. Visceral signals shape brain dynamics and cognition. Trends Cogn Sci 2019;23(6):488–509.
Basha D, Chauvette S, Sheroziya M, Timofeev I. Respiration organizes gamma synchrony in the prefronto-thalamic network. Sci Rep 2023;13(1):8529.
Bastuji H, García-Larrea L. Evoked potentials as a tool for the investigation of human sleep. Sleep Med Rev 1999;3(1):23–45.
Beas BS, Wright BJ, Skirzewski M, Leng Y, Hyun JH, Koita O, et al. The locus coeruleus drives disinhibition in the midline thalamus via a dopaminergic mechanism. Nat Neurosci 2018;21(7):963–73.
Bonnefond M, Kastner S, Jensen O. Communication between brain areas based on nested oscillations. eNeuro 2017;4(2).
Boutin A, Doyon J. A sleep spindle framework for motor memory consolidation. Philos Trans R Soc Lond B Biol Sci 2020;375(1799):20190232.
Boutin A, Gabitov E, Pinsard B, Boré A, Carrier J, Doyon J. Clustering and temporal organization of sleep spindles underlie motor memory consolidation. bioRxiv 2022:2022.11.29.518200.
Brændholt M, Kluger DS, Varga S, Heck DH, Gross J, Allen MG. Breathing in waves: Understanding respiratory-brain coupling as a gradient of predictive oscillations. Neurosci Biobehav Rev 2023;152 105262.
Canolty RT, Knight RT. The functional role of cross-frequency coupling. Trends Cogn Sci 2010;14(11):506–15.
Clemens Z, Molle M, Eross L, Barsi P, Halasz P, Born J. Temporal coupling of parahippocampal ripples, sleep spindles and slow oscillations in humans. Brain 2007;130(Pt 11):2868–78.
Contreras D, Steriade M. Cellular basis of EEG slow rhythms: a study of dynamic corticothalamic relationships. J Neurosci 1995;15(1 Pt 2):604–22.

Ding L, Chen B, Dai Y, Li Y. A meta-analysis of the first-night effect in healthy individuals for the full age spectrum. Sleep Med 2022;89:159–65.
Driver HS, Dijk DJ, Werth E, Biedermann K, Borbély AA. Sleep and the sleep electroencephalogram across the menstrual cycle in young healthy women. J Clin Endocrinol Metab 1996;81(2):728–35.
Fell J, Axmacher N. The role of phase synchronization in memory processes. Nat Rev Neurosci 2011;12(2):105–18.
Fernandez LMJ, Luthi A. Sleep spindles: mechanisms and functions. Physiol Rev 2020;100(2):805–68.
Fogel SM, Smith CT. The function of the sleep spindle: a physiological index of intelligence and a mechanism for sleep-dependent memory consolidation. Neurosci Biobehav Rev 2011;35(5):1154–65.
Foglia L, Wilson RA. Embodied cognition. Wiley Interdiscip Rev Cogn Sci 2013;4 (3):319–25.
Folschweiller S, Sauer JF. Phase-specific pooling of sparse assembly activity by respiration-related brain oscillations. J Physiol 2022;600(8):1991–2011.
Folschweiller S, Sauer JF. Controlling neuronal assemblies: a fundamental function of respiration-related brain oscillations in neuronal networks. Pflugers Arch 2023;475(1):13–21.
Fontanini A, Spano P, Bower JM. Ketamine-xylazine-induced slow (< 1.5 Hz) oscillations in the rat piriform (olfactory) cortex are functionally correlated with respiration. J Neurosci 2003;23(22):7993–8001.
Girin B, Juventin M, Garcia S, Lefevre L, Amat C, Fourcaud-Trocme N, et al. The deep and slow breathing characterizing rest favors brain respiratory-drive. Sci Rep 2021;11(1):7044.
Grosmaitre X, Santarelli LC, Tan J, Luo M, Ma M. Dual functions of mammalian olfactory sensory neurons as odor detectors and mechanical sensors. Nat Neurosci 2007;10(3):348–54.
Grund M, Al E, Pabst M, Dabbagh A, Stephani T, Nierhaus T, et al. Respiration, heartbeat, and conscious tactile perception. J Neurosci 2022;42(4):643–56.
Hammer M, Schwale C, Brankack J, Draguhn A, Tort ABL. Theta-gamma coupling during REM sleep depends on breathing rate. Sleep 2021;44(12).
Heck DH, Correia BL, Fox MB, Liu Y, Allen M, Varga S. Recent insights into respiratory modulation of brain activity offer new perspectives on cognition and emotion. Biol Psychol 2022;170 108316.
Heck DH, Kozma R, Kay LM. The rhythm of memory: how breathing shapes memory function. J Neurophysiol 2019;122(2):563–71.
Heck DH, McAfee SS, Liu Y, Babajani-Feremi A, Rezaie R, Freeman WJ, et al. Breathing as a fundamental rhythm of brain function. Front Neural Circuits 2016;10:115.
Herrero JL, Khuvis S, Yeagle E, Cerf M, Mehta AD. Breathing above the brain stem: volitional control and attentional modulation in humans. J Neurophysiol 2018;119(1):145–59.
Ito J, Roy S, Liu Y, Cao Y, Fletcher M, Lu L, et al. Whisker barrel cortex delta oscillations and gamma power in the awake mouse are linked to respiration. Nat Commun 2014;5:3572.
Johannknecht M, Kayser C. The influence of the respiratory cycle on reaction times in sensory-cognitive paradigms. Sci Rep 2022;12(1):2586.
Jung F, Yanovsky Y, Brankack J, Tort ABL, Draguhn A. Respiratory entrainment of units in the mouse parietal cortex depends on vigilance state. Pflugers Arch 2022.
Jung F, Yanovsky Y, Brankačk J, Tort ABL, Draguhn A. Respiratory entrainment of units in the mouse parietal cortex depends on vigilance state. Pflugers Arch 2023;475(1):65–76.
Juventin M, Ghibaudo V, Granget J, Amat C, Courtiol E, Buonviso N. Respiratory influence on brain dynamics: the preponderant role of the nasal pathway and deep slow regime. Pflugers Arch 2022.
Juventin M, Ghibaudo V, Granget J, Amat C, Courtiol E, Buonviso N. Respiratory influence on brain dynamics: the preponderant role of the nasal pathway and deep slow regime. Pflugers Arch 2023;475(1):23–35.
Karalis N, Sirota A. Breathing coordinates cortico-hippocampal dynamics in mice during offline states. Nat Commun 2022;13(1):467.
Klinzing JG, Niethard N, Born J. Mechanisms of systems memory consolidation during sleep. Nat Neurosci 2019;22(10):1598–610.
Kluger DS, Forster C, Abbasi O, Chalas N, Villringer A, Gross J. Modulatory dynamics of periodic and aperiodic activity in respiration-brain coupling. Nat Commun 2023;14(1):4699.
Kluger DS, Gross J. Depth and phase of respiration modulate cortico-muscular communication. NeuroImage 2020;222 117272.
Kluger DS, Gross J. Respiration modulates oscillatory neural network activity at rest. PLoS Biol 2021;19(11):e3001457.
Landler L, Ruxton GD, Malkemper EP. The Hermans-Rasson test as a powerful alternative to the Rayleigh test for circular statistics in biology. BMC Ecology 2019;19(1):30.
Latchoumane C-FV, Ngo H-VV, Born J, Shin H-S. Thalamic spindles promote memory formation during sleep through triple phase-locking of cortical, thalamic, and hippocampal rhythms. Neuron 2017;95(2):424–435.e6.
Lázár ZI, Dijk DJ, Lázár AS. Infraslow oscillations in human sleep spindle activity. Journal of neuroscience methods 2019;316:22–34.
Lecci S, Fernandez LM, Weber FD, Cardis R, Chatton JY, Born J, et al. Coordinated infraslow neural and cardiac oscillations mark fragility and offline periods in mammalian sleep. Sci Adv 2017;3(2) e1602026.
Lechinger J, Heib DP, Gruber W, Schabus M, Klimesch W. Heartbeat-related EEG amplitude and phase modulations from wakefulness to deep sleep: interactions with sleep spindles and slow oscillations. Psychophysiology 2015;52 (11):1441–50.
Liu Y, McAfee SS, Heck DH. Hippocampal sharp-wave ripples in awake mice are entrained by respiration. Sci Rep 2017;7(1):8950.
Macnutt MJ, De Souza MJ, Tomczak SE, Homer JL, Sheel AW. Resting and exercise ventilatory chemosensitivity across the menstrual cycle. J Appl Physiol 2012,;112(5):737–47.
Mizuhara K, Nittono H. Visual discrimination accuracy does not differ between nasal inhalation and exhalation when stimuli are voluntarily aligned to breathing phase. Int J Psychophysiol 2022;173:1–8.
Mizuhara K, Nittono H. Effects of respiratory phases on the processing of emotional and non-emotional visual stimuli. Psychophysiology 2023;60(6) e14261.
Nakamura NH, Fukunaga M, Oku Y. Respiratory modulation of cognitive performance during the retrieval process. PLoS One 2018;13(9) e0204021.
Nikolaev YA, Dosen PJ, Laver DR, van Helden DF, Hamill OP. Single mechanically-gated cation channel currents can trigger action potentials in neocortical and hippocampal pyramidal neurons. Brain Res 2015;1608:1–13.
Parviainen T, Lyyra P, Nokia MS. Cardiorespiratory rhythms, brain oscillatory activity and cognition: review of evidence and proposal for significance. Neurosci Biobehav Rev 2022;142 104908.
Perl O, Ravia A, Rubinson M, Eisen A, Soroka T, Mor N, et al. Human non-olfactory cognition phase-locked with inhalation. Nat Hum Behav 2019;3(5):501–12.
Pollatos O, Schandry R. Accuracy of heartbeat perception is reflected in the amplitude of the heartbeat-evoked brain potential. Psychophysiology 2004;41 (3):476–82.
Purcell SM, Manoach DS, Demanuele C, Cade BE, Mariani S, Cox R, et al. Characterizing sleep spindles in 11,630 individuals from the National Sleep Research Resource. Nat Commun 2017;8:15930.
Rassler B, Raabe J. Co-ordination of breathing with rhythmic head and eye movements and with passive turnings of the body. Eur J Appl Physiol 2003;90(1–2):125–30.
Roux SG, Garcia S, Bertrand B, Cenier T, Vigouroux M, Buonviso N, et al. Respiratory cycle as time basis: an improved method for averaging olfactory neural events. Journal of neuroscience methods 2006;152(1–2):173–8.
Schreiner T, Petzka M, Staudigl T, Staresina BP. Endogenous memory reactivation during sleep in humans is clocked by slow oscillation-spindle complexes. Nat Commun 2021;12(1):3112.
Schreiner T, Petzka M, Staudigl T, Staresina BP. Respiration shapes sleep-oscillations and memory reactivation in humans. bioRxiv 2023:2023.03.16.532910.
Sliwa J. Toward collective animal neuroscience. Science 2021;374(6566):397–8.
Staresina BP, Bergmann TO, Bonnefond M, van der Meij R, Jensen O, Deuker L, et al. Hierarchical nesting of slow oscillations, spindles and ripples in the human hippocampus during sleep. Nat Neurosci 2015;18(11):1679–86.
Tort ABL, Brankack J, Draguhn A. Respiration-entrained brain rhythms are global but often overlooked. Trends Neurosci 2018;41(4):186–97.
Tort ABL, Hammer M, Zhang J, Brankack J, Draguhn A. Temporal relations between cortical network oscillations and breathing frequency during REM sleep. J Neurosci 2021;41(24):5229–42.
Vallat R, Walker MP. An open-source, high-performance tool for automated sleep staging. Elife 2021:10.
Varga S, Heck DH. Rhythms of the body, rhythms of the brain: respiration, neural oscillations, and embodied cognition. Conscious Cogn 2017;56:77–90.
Watanabe T, Itagaki A, Hashizume A, Takahashi A, Ishizaka R, Ozaki I. Observation of respiration-entrained brain oscillations with scalp EEG. Neurosci Lett 2023;797 137079.
West JB, Luks AM. West's respiratory physiology. The Essentials: Wolters Kluwer; .
Yackle K, Schwarz LA, Kam K, Sorokin JM, Huguenard JR, Feldman JL, et al. Breathing control center neurons that promote arousal in mice. Science 2017;355 (6332):1411–5.
Yang CF, Feldman JL. Efferent projections of excitatory and inhibitory preBötzinger Complex neurons. J Comp Neurol 2018;526(8):1389–402.
Zelano C, Jiang H, Zhou G, Arora N, Schuele S, Rosenow J, et al. Nasal respiration entrains human limbic oscillations and modulates cognitive function. J Neurosci 2016;36(49):12448–67.